Journal of Power Sources 196 (2011) 3009–3014

Contents lists available at ScienceDirect

Journal of Power Sources

journal homepage: www.elsevier.com/locate/jpowsour

Polymer coatings as separator layers for microbial fuel cell cathodes

Valerie J. Watson[a], Tomonori Saito[a,b], Michael A. Hickner[b], Bruce E. Logan[a,*]

[a] Department of Civil and Environmental Engineering, The Pennsylvania State University, University Park, PA 16802, USA
[b] Department of Material Science and Engineering, The Pennsylvania State University, University Park, PA 16802, USA

ARTICLE INFO

Article history:
Received 3 September 2010
Received in revised form
10 November 2010
Accepted 22 November 2010
Available online 27 November 2010

Keywords:
Microbial fuel cell
Cathode
Membrane
Anion exchange
Cation exchange

ABSTRACT

Membrane separators reduce oxygen flux from the cathode into the anolyte in microbial fuel cells (MFCs), but water accumulation and pH gradients between the separator and cathode reduces performance. Air cathodes were spray-coated (water-facing side) with anion exchange, cation exchange, and neutral polymer coatings of different thicknesses to incorporate the separator into the cathode. The anion exchange polymer coating resulted in greater power density ($1167 \pm 135\ mW\ m^{-2}$) than a cation exchange coating ($439 \pm 2\ mW\ m^{-2}$). This power output was similar to that produced by a Nafion-coated cathode ($1114 \pm 174\ mW\ m^{-2}$), and slightly lower than the uncoated cathode ($1384 \pm 82\ mW\ m^{-2}$). Thicker coatings reduced oxygen diffusion into the electrolyte and increased coulombic efficiency (CE = 56–64%) relative to an uncoated cathode ($29 \pm 8\%$), but decreased power production ($255–574\ mW\ m^{-2}$). Electrochemical characterization of the cathodes *ex situ* to the MFC showed that the cathodes with the lowest charge transfer resistance and the highest oxygen reduction activity produced the most power in MFC tests. The results on hydrophilic cathode separator layers revealed a trade off between power and CE. Cathodes coated with a thin coating of anion exchange polymer show promise for controlling oxygen transfer while minimally affecting power production.

1. Introduction

Microbial fuel cells (MFCs) represent one of the latest innovations for the treatment of wastewater streams in combination with electricity production [1]. Typical MFCs consist of a microbe-enriched anode where organic matter is oxidized. Electrons are conducted through a circuit to the air-fed cathode consisting of a porous carbon structure with platinum catalyst, where oxygen is reduced to water [2]. Some MFCs include an ion exchange membrane in the electrolyte compartment between the anode and cathode. However, membranes have been shown to negatively impact the power production of the MFC by increasing the internal resistance of the cell and inducing pH gradients during cell operation [3,4]. MFC power production can be improved by removing the membrane from the system [5] and reducing the electrode spacing to decrease ohmic losses. When the electrodes become closely spaced, however, a separator is needed to prevent short circuiting and also to reduce oxygen diffusion into the anode chamber which can adversely affect power production [1,6].

The performance characteristics of membrane separators have been investigated in bioelectrochemical systems, including cation exchange (CEM), anion exchange (AEM), bipolar, and ultrafiltration membranes [4,7–10]. It has been shown that the cations (Na^+, K^+, and NH_4^+) are preferentially transferred through the CEM due to their high concentrations rather than protons to maintain charge balance, and as a result there is a decrease in performance due to pH changes [3,11]. AEMs outperform CEMs and other types of membranes in MFCs and microbial electrolysis cells (MECs) mostly due to lower internal resistances that result from lower charge transport resistance [4,8,9,12]. Charge balance can be facilitated by transfer of buffer anions (such as phosphate) when using an AEM [4]. However, both AEMs and CEMs negatively impact microbial fuel cell performance due to the formation of a pH gradient at the electrodes [7].

Oxygen diffusion into the anode chamber negatively affects MFC performance by serving as an alternative electron acceptor for the facultative bacteria at the anode. If the bacteria use the oxygen as the terminal electron acceptor instead of the anode current collector, the coulombic efficiency (CE) will decrease, the anode potential will become more positive, and the current density will decrease [13]. Cloth (J-cloth) separators have been used to decrease oxygen diffusion into the anolyte, but over time the cloth became completely degraded by the bacteria in the reactor [14,15]. Positioning a glass fiber separator next to the cathode in an MFC with 2 cm electrode spacing has been shown to increase CE to 80% compared to 30% without a separator [14]. Power production with the separator decreased from $896\ mW\ m^{-2}$ to $791\ mW\ m^{-2}$ as a result of decreased cathode potential and increased ohmic resis-

* Corresponding author at: Department of Civil and Environmental Engineering, The Pennsylvania State University, 212 Sackett Building, University Park, PA 16802, USA. Tel.: +1 814 863 7908; fax: +1 814 863 7304.
E-mail address: blogan@psu.edu (B.E. Logan).

0378-7753/$ – see front matter © 2010 Elsevier B.V. All rights reserved.
doi:10.1016/j.jpowsour.2010.11.105

tance. To improve power production, the electrode spacing was decreased using the separator which prevented short-circuiting. With the decreased electrode spacing, the power density increased to 1195 mW m^{-2} while maintaining CE at 80%. In the same study, growth of biofilm on the cathode was also found to improve CE over time due to a decrease in oxygen diffusion into the electrolyte from the air cathode, but the biofilm also hindered proton migration to the cathode and limited power production [14].

Zhang et al. [16] placed AEMs and CEMs in the electrolyte compartment directly adjacent to the cathode and obtained around 90% CE. However, the membranes deformed after several cycles due to membrane swelling during ion and water transport, and the deformation created a void space between the membrane and electrode filled with water and gas. The water trapped between the membrane and the cathode had a higher pH than the anode chamber and decreased the cathode potential. The researchers used stainless steel mesh to keep the membrane pressed against the cathode and prevent water accumulation behind the membrane. In this configuration, the ohmic resistance of the reactor decreased from 120 Ω to 15 Ω with the AEM and from 49 Ω to 16 Ω with the CEM, while the power density increased from 16 W m^{-3} to 46 W m^{-3} with the AEM and from 21 W m^{-3} to 32 W m^{-3} with the CEM [16]. In previous studies when Nafion was hot-pressed on to carbon cloth preventing deformation, the CE increased from 9–12% to 40–50%, but the power density decreased from 12.5 W m^{-3} to 6.6 W m^{-3} [5]. Hot pressing the membrane to the cathode decreased the power by increasing the ohmic resistance of the membrane, likely due to adverse effects of the bonding process on membrane permeability [4]. Therefore, it is important to incorporate the membrane into the cathode to prevent deformation while also striving to minimize the ohmic resistance of the membrane.

In next-generation MFC systems, a separator between the anode and cathodes will be important to facilitate minimum electrode spacing while preventing short circuiting of the electrodes [1]. The separators must limit oxygen diffusion to the anolyte while not impeding proton transfer to the cathode catalyst. This study explored the use of spray coating for applying a thin layers of hydrophilic cation exchange, anion exchange, and neutral polymers to the electrolyte side of the cathode structure and measured the layers' effect on power production and CE with respect to polymer type, oxygen diffusivity, and biofilm growth at the cathode.

2. Materials and methods

2.1. Polymers

Bisphenol A-based poly(sulfone) (Udel P-3500 LCD, M_w 79,000 g mol^{-1}, 1.24 g cm^{-3}) and poly(phenylsulfone) (Radel R-5500, M_w 63,000 g mol^{-1}, 1.29 g cm^{-3}) were kindly donated by Solvay Advanced Polymers, LLC. Radel was aminated (A-Radel, ion exchange capacity of IEC = 2.64 meq g^{-1}) or sulfonated (S-Radel, IEC = 2.54 meq g^{-1}) as previously described [17–19]. Nafion solution (Nafion® 117 solution), ~5 wt% in a mixture of lower aliphatic alcohols and water was purchased from Aldrich and used as received. Poly(styrene)-*b*-poly(ethylene oxide) diblock copolymer PS_{156}-*b*-PEO_{110} (PEO110, M_n 21,100 g mol^{-1}, M_w/M_n = 1.01) was synthesized as previously described [20], where subscripted numbers denote the corresponding number of repeat units of each block. Polymer solutions (5 wt%) were prepared by dissolving Udel and PEO-110 in tetrahydrofuran and A-Radel and S-Radel in methanol. Properties of each of the polymers are summarized in Table 1.

2.2. Cathode construction

Platinum-catalyzed air cathodes (projected surface area of 7 cm^2) were constructed from carbon cloth containing 30 wt% wet proofing polymer (#B1B30WP, BASF Corp.) with PTFE diffusion layers, and 0.5 mg-Pt cm^{-2} catalyst loading [21]. The polymer layers were applied to the cathodes in layers using an air brush (Paache, BearAir, S. Easton, MA). The sprayed polymer coating was allowed to dry between layers and then checked for resistivity using a handheld digital multimeter (Model 83 III, Fluke) and weighed to determine the amount of coating applied (Table 1). Once coated, all cathode surfaces produced a resistance greater than the measurement range of the multimeter, effectively electrically insulating the electrolyte-facing surface of the cathode. Two cathodes were coated for each polymer tested. The average wet and dry thicknesses of the coatings were calculated from the measured mass of the applied polymer, the density of the dry polymer, and the polymer's water uptake (Table 1). The thicknesses of the polymer layers applied to the solution side of the cathode structure are included in the names of the samples as indicated by the number to the right of the dash, for instance A-Radel-146 indicates that the A-Radel coating on those cathodes averaged 146 μm in thickness.

2.3. MFC reactor construction and operation

Cube-shaped MFCs were constructed as previously described [5]. The anode chamber was a 28 mL cylindrical chamber (7 cm^2 cross section) bored into a Lexan block. The brush anode was constructed from carbon fibers (PANEX®33 160K, ZOLTEK) wound into a titanium wire core (2.5 cm diameter, 2.5 cm length, and 0.22 m^2 surface area) which was heat treated at 450 °C [22] then placed horizontally in the center of the cylinder. The electrode spacing was 2.5 cm (center of the anode to the face of the cathode).

Effluent from the anode chamber of an enriched MFC operated under similar conditions to those in this study was used for the mixed culture inoculum. The medium used in MFC performance tests was a 100 mM phosphate buffer solution (PBS) (9.125 g L^{-1} Na_2HPO_4, 4.904 g L^{-1} $NaH_2PO_4 \cdot H_2O$, 0.31 g L^{-1} NH_4Cl, and 0.13 g L^{-1} KCl; pH 7) with vitamins and minerals [23] and 1 g L^{-1} sodium acetate. The PBS concentration was doubled to 200 mM in tests where indicated. MFCs were inoculated with a 50% (v v^{-1}) inoculum of effluent and medium and were covered

Table 1
Properties of polymers and cathode coatings.

Cathode	Type	IEC (meq g^{-1})	IEC_v (wet) (meq cm^{-3})	Water uptake	Solvent	Density (g cm^{-3})	Weight (mg)	Thickness (dry) (μm)	Thickness (wet) (μm)
Nafion-62	CEM	0.91	1.59	20%	Aliph-Alc	2.10	122.3 ± 0.8	52 ± 0.3	62 ± 0.4
A-Radel-146	AEM	2.64	1.22	180%	MeOH	1.29	75.8 ± 0.1	52 ± 0.0	146 ± 0.0
A-Radel-67	AEM	2.64	1.22	180%	MeOH	1.29	34.7 ± 4.5	24 ± 1.9	67 ± 2.3
S-Radel-60	CEM	2.54	1.93	70%	MeOH	1.29	51.7 ± 0.7	35 ± 0.3	60 ± 0.4
S-Radel-47	CEM	2.54	1.93	70%	MeOH	1.29	40.7 ± 1.0	28 ± 0.4	47 ± 0.5
PEO110-101	N-Phil[a]	0	0	50%	THF	1.10	83.8 ± 6.6	67 ± 2.8	101 ± 3.4
Udel-32	N-Phob[b]	0	0	0%	THF	1.24	44.5 ± 2.8	32 ± 1.2	32 ± 1.4

[a] Neutral – hydrophilic polymer.
[b] Neutral – hydrophobic polymer.

to exclude light. The electrodes were connected through a 1000 Ω resistor, except as noted. Once an MFC produced ≥100 mV, no additional inoculum was added to the medium over subsequent fed batch cycles. All MFCs were operated at 30 °C in a controlled-climate room. The MFCs were considered enriched and ready for testing once they achieved the same maximum voltage for three consecutive batch cycles. Once the MFC anodes were enriched, the uncoated cathodes used for startup were removed and the coated cathodes and new uncoated cathodes were placed in the reactors. All MFC tests were conducted with duplicate cathodes and averages over two cycles were reported with standard deviations for $n = 4$ (two cathodes over two cycles), except for CE which was averaged from duplicate reactors over three cycles ($n = 6$).

2.4. Analysis

The voltage across the resistor was recorded every 30 min using a multimeter (model 2700 Keithley Instruments, Cleveland, OH) with a computerized data acquisition system. Polarization curves were obtained by applying a different external resistance to the circuit for a complete batch cycle and the maximum sustainable voltage (typically sustained for 7–30 h depending on the total length of the cycle) was recorded for each resistance. Current density was calculated from $I = E/R$, where I is the current, E the measured voltage, and R the external resistance, and normalized to the projected cathode surface area. Power densities were calculated using $P = IE$, and normalized by the projected cathode surface area [24].

CE was calculated from the ratio of the total electrical charge produced during the experiment (at 1000 Ω) to the theoretical amount of electrons available from the oxidation of acetate to carbon dioxide. Therefore, CE $[\%] = (C_{Ex}/C_{Th}) \times 100$, where $C_{Ex} = \sum_{t=1}^{T}(E_i t_i)/R$, $C_{Th} = FbMv$, F is Faraday's constant (96,485 C mol e^{-1}), b is the number of moles of electrons available per mole of substrate (8 mol e (mol acetate)$^{-1}$), M is the acetate concentration (mol L^{-1}), and v is the volume of liquid in the anode chamber (L) [24].

The oxygen flux into the electrolyte chamber through each cathode was calculated by measuring the change in dissolved oxygen concentration (NeoFox, Ocean Optics Inc., FL) over time in a stirred abiotic MFC reactor (30 mL) without an active anode as previously described [4].

The impedance of each cathode half-cell was measured by electrochemical impedance spectroscopy (EIS) at 0.1 V (vs. Ag/AgCl) over a frequency of 100,000–0.1 Hz with sinusoidal perturbation of 10 mV using a potentiostat (PC 4/750, Gamry Instrument Inc.) at 30 °C. The half-cell consisted of a 7 cm^2 platinum disk counter electrode set parallel to the test cathode and equipped with an Ag/AgCl reference electrode (+0.2 V vs. NHE) (RE-5B, BASI, IN). The test cell was filled with 200 mM PBS (13 mL, pH 7) without substrate or other nutrients. The combined solution and membrane resistances ($R_s + R_m$) were obtained from Nyquist impedance plots at the point where Z_{imag} was equal to zero at high frequency. The charge transfer resistance (R_{ct}) for each cathode was estimated from a semi-circular fit of the charge transfer impedance in the Nyquist plot [25,26].

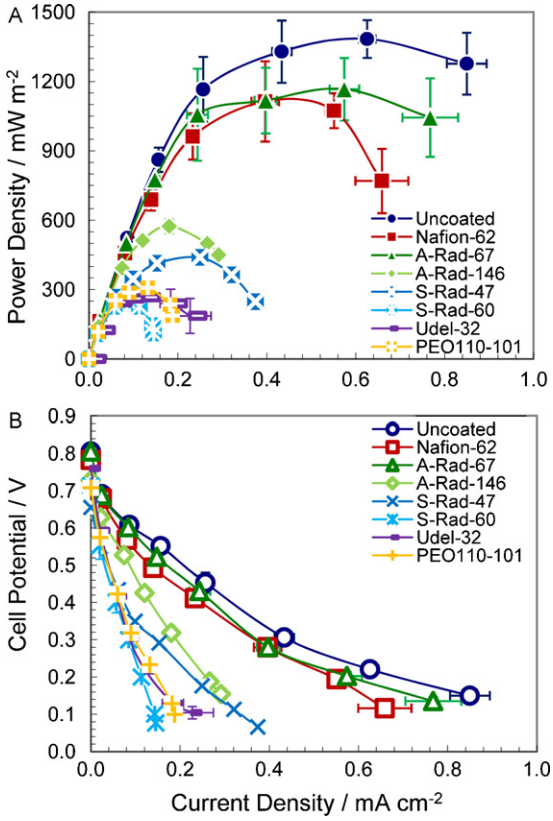

Fig. 1. (A) Power density and (B) polarization curves for polymer-coated cathodes.

The oxygen reduction response of each cathode was measured by linear sweep voltammetry (LSV) using the same experimental setup as with EIS at a scan rate of 1 mV s^{-1} over the range of 0.6 to −0.3 V (vs. Ag/AgCl) with current interrupt correction. The oxygen reduction activity of the cathodes was measured in both 200 mM and 100 mM PBS solution (pH 7).

3. Results

3.1. MFC performance

MFCs with cathodes coated with a thin layer of anion exchange polymer (A-Radel-67) produced approximately the same maximum power (Table 2) as the cells with cathodes coated with Nafion of similar thickness (Nafion-62) (Fig. 1). MFC tests with uncoated cathodes resulted in slightly higher power density than Nafion-62 or A-Radel-67 coated cathodes. MFCs with cation exchange Radel polymer coatings on the cathode (S-Radel-47) produced much less power than the cells with the uncoated control cathodes, as did reactors with thin layers of Udel hydrophobic polymer, Udel-32. The A-Radel-146 and S-Radel-60 coated cathodes had thicker coatings and produced less power than the cathodes coated with a

Table 2
Oxygen flux, combined solution and membrane resistance, charge transfer resistance, and maximum power density of cathodes.

Cathode	Oxygen flux (mg cm^{-2} h^{-1})	$R_s + R_m$ (Ω)	R_{ct} (Ω)	Maximum power density (mW m^{-2})
Uncoated	0.055	5	19	1384 ± 82
Nafion-62	0.022	7	57	1114 ± 174
A-Radel-146	0.010	7	85	574 ± 32
A-Radel-67	.023	7	22	1167 ± 135
S-Radel-60	0.004	9	>100	255 ± 28
S-Radel-47	0.012	7	>100	439 ± 2
PEO110-101	0.002	7	>100	307 ± 9
Udel-32	0.008	18	>100	266 ± 16

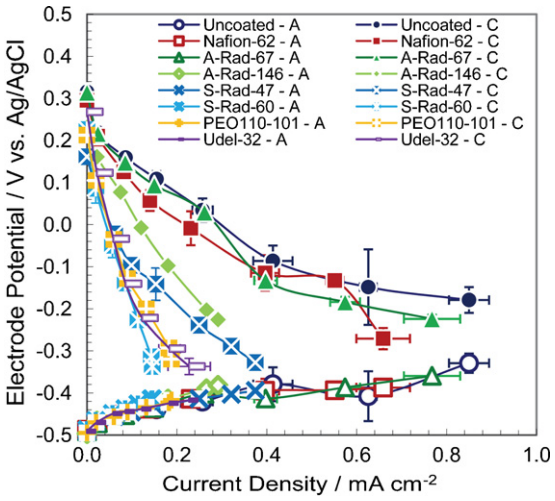

Fig. 2. Electrode potential measurements (vs. Ag/AgCl) during cell polarization.

thinner layer of the same polymer (A-Radel-67 and S-Radel-47), most likely due to increased impedance of proton transfer. The observed differences in power production during polarization were due to differences in cathode potentials (Fig. 2) since anode potentials did not vary over the current density range tested.

The CEs of the MFCs ranged between 29% and 64% (Fig. 3; fixed external resistance of 1000 Ω). Cathodes with thicker coatings of the same polymer type had higher CEs (A-Radel-146, 56 ± 2%; S-Radel-60, 64 ± 5%) than the cathodes with thinner coatings (A-Radel-67, 33 ± 8%; S-Radel-47, 40 ± 10%).

3.2. Electrochemical performance

The A-Radel-67 cathode had the lowest impedance ($R_s + R_m = 7\ \Omega$ and $R_{ct} = 22\ \Omega$) of all the coated cathodes (Fig. 4 and Table 2) and only slightly higher resistances than the uncoated cathode ($R_s + R_m = 5\ \Omega$ and $R_{ct} = 19\ \Omega$). Since R_m is zero for the uncoated cathode, R_s is 5 Ω for the half-cell control geometry used in these experiments. Thus, for all coated cathodes except Udel-32, the coating added an R_m of between 2 and 4 Ω. However, larger effects of the coatings can be observed in the R_{ct}, most likely due to the decrease of reactant concentration at the catalyst or a decrease in available catalyst sites. A-Radel-67 had the smallest increase in R_{ct} (+3 Ω) compared to the uncoated cathode while Nafion-62 showed an R_{ct} of 38 Ω greater than the uncoated control cathode.

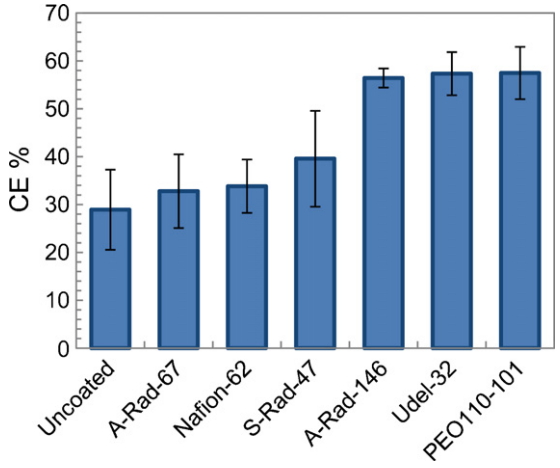

Fig. 3. Coulombic efficiencies for cycles run at 1000 Ω.

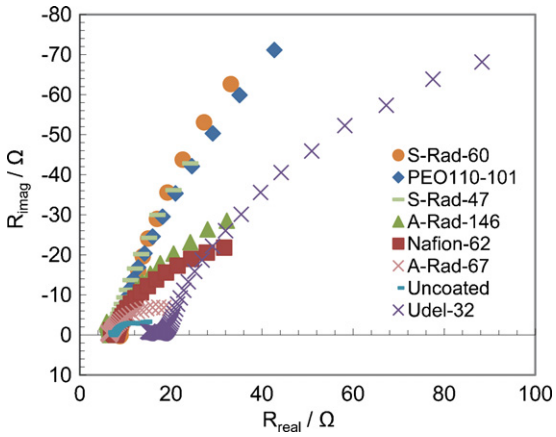

Fig. 4. EIS of coated and uncoated cathodes at 0.1 V (vs. Ag/AgCl) (200 mM PBS).

S-Radel-60, S-Radel-47, PEO110-101, and Udel-32 coated cathodes had R_{ct} values of greater than 100 Ω.

The effect of the coatings on the oxygen reduction performance of the cathodes can be observed by the decrease in current density during LSV testing compared to the uncoated control (Fig. 5). The current densities obtained from LSV for each coated cathode showed the same trends as power production in MFC tests. For example, A-Radel-67 produced higher current densities in LSV and the maximum power in the MFC tests, and S-Radel-60 and Udel-32 produced the lowest current densities in LSV and the lowest power densities. LSV showed similar trends between cathodes using either the 100 mM PBS or 200 mM PBS solution.

3.3. Oxygen diffusion and biofilm growth

The coatings applied to the cathode decreased the rate of oxygen diffusion into the anode solution as demonstrated by the measured oxygen flux into the electrolyte compartment (Table 2). The decrease in oxygen diffusion was not exclusively a function of the amount of polymer applied (i.e., the thickness or the weight of the coating), but was a combined result of the type of polymer, the processing of the layer (e.g. solvent used for coating deposition), and the coating thickness on the cathode. The oxygen flux was inversely related to the CE during MFC testing. The cathodes with the highest rate of oxygen diffusion and the lowest CE developed a significant layer of biofilm after 100 days of operation (Fig. 6). S-Radel-60,

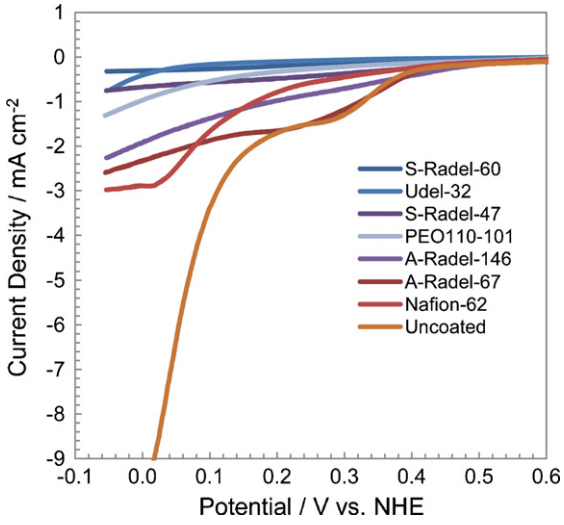

Fig. 5. LSV of coated and uncoated cathodes (100 mM PBS).

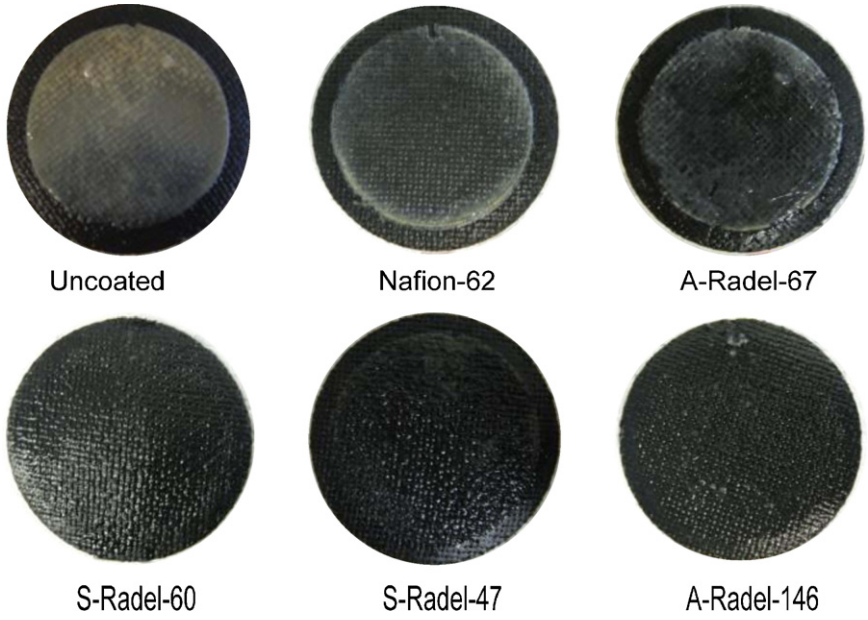

Fig. 6. Optical images of biofilm growth on cathodes (100 days).

PEO110-101, A-Radel-60, and Udel-32 cathodes did not develop a visible biofilm layer.

4. Discussion

Of the coated cathodes, the MFCs using the A-Radel-67 cathodes produced the highest power density. In general, MFCs that had cathodes with the lowest R_{ct} achieved the highest power density (Fig. 7). The A-Radel (AEM) had a lower R_{ct} and higher power production than both of the CEMs (S-Radel and Nafion). The better performance of the A-Radel is consistent with results in previous studies comparing AEM and CEM separators in MFCs [4,8] which indicate phosphate anions buffer pH changes and maintain charge balance. We therefore conclude that positively charged quaternary ammonium groups on the AEM layer aid anion transport and result in less accumulation of cations compared to CEM layers. The preferential anion transport in AEMs may also decrease the pH gradient toward the catalyst moiety compared to that of CEM layers [9]. The AEM had higher water uptake than the CEM when comparing similar IECs and polymer backbones (i.e. A-Radel and S-Radel). The higher water uptake of the AEM likely decreased its ion transport resistance which could have also contributed to the higher power density output of AEM coating than that of the CEM coating.

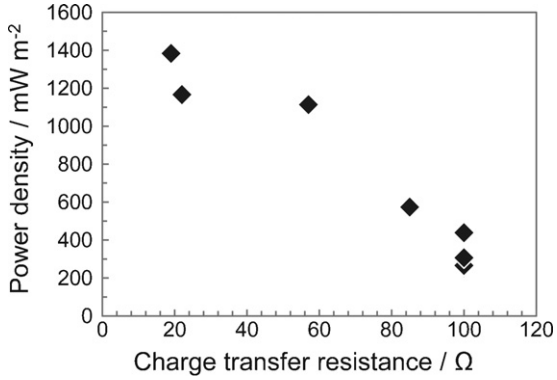

Fig. 7. Inverse relationship between R_{ct} and power density.

Although S-Radel and Nafion are both CEMs, the S-Radel hindered power production more than the Nafion coating of the same thickness, which is reflected in the increase in R_{ct}. The greater R_{ct} can be explained by considering the IEC_v, the volumetric concentration of ions in the swollen polymer. The S-Radel had a higher IEC_v than Nafion and as seen in previous studies, the higher IEC_v can impede proton diffusion at neutral pH [19]. Sulfonate groups in the CEM layers were most likely saturated with Na^+ and K^+ rather than H^+ due to the high Na^+ and K^+ concentration in the electrolyte. The accumulated cations hindered proton diffusion through the CEM layer on the cathode and within the electrode where the layers had penetrated the porous structure. It is also possible that polymer seepage into the cathode pores inhibited oxygen transport to the catalyst surface, which increased R_{ct}. R_{ct} of the A-Radel cathodes increased and the corresponding maximum power density decreased as the applied layer thickness increased and the same effect was observed for the S-Radel cathodes.

The uncharged, hydrophilic polymer coatings of PEO110 had a greater R_{ct} than the A-Radel coating of similar thickness (A-Radel-146 compared to PEO110-101, and A-Radel-67 compared to Udel-32), most likely due to the A-Radel coating having a greater water uptake (Table 1) and therefore less impedance to proton transfer. The significant increase in R_{ct} for PEO110-101, with a reasonably high water uptake, implies that anion transport to decrease the pH gradient in an AEM may be an important factor in the resulting R_{ct}.

In general, there was an inverse relationship between the maximum power density and CE (Fig. 8), except for the S-Radel-47, which had a lower power density ($440 \pm 4\,mW\,m^{-2}$) and lower CE ($40 \pm 10\%$) than the A-Radel-146 ($574 \pm 32\,mW\,m^{-2}$ and $CE = 56 \pm 2\%$). The cathode coatings with lower oxygen permeability did not show an improvement in anode potential resulting from a decrease in oxygen intrusion, most likely due to biofilm formation on coatings with higher oxygen permeability, which limited oxygen diffusion to the anode. The biofilm formation on the cathodes with higher oxygen permeability was most likely the cause of the decrease in CE compared to the less permeable cathodes. Despite similar anode performance, the cathodes with less oxygen permeability and higher CE produced less power due to an increase in R_{ct} caused by the increased resistance of the coatings to either proton or oxygen diffusion to the catalyst surface.

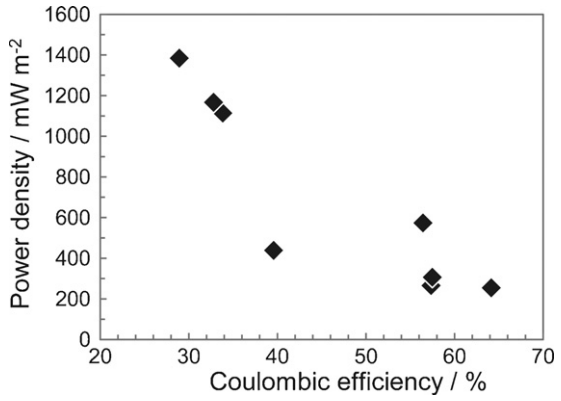

Fig. 8. Inverse relationship between CE and power density.

Polymer coated cathodes can be useful in MFC designs as further efforts are made to develop polymer coatings that facilitates proton transfer to the cathode but limit oxygen diffusion into the electrolyte and provide an electrically insulating surface. Anion exchange polymers such as A-Radel, integrated as a thin membrane coating into MFC cathodes, have potential for controlling oxygen diffusion into the MFC while minimally affecting power production.

Acknowledgements

This research was supported under a National Science Foundation Graduate Research Fellowship, National Science Foundation Grant CBET-0730359, and the King Abdullah University of Science and Technology (KAUST) (Award KUS-I1-003-13). Thanks to Solvay Advanced Polymers for the donation of Radel® and Udel® polymer and to Justin Tokash for insights into EIS theory and application.

References

[1] B. Logan, Appl. Microbiol. Biotechnol. 85 (2010) 1665–1671.
[2] B.E. Logan, Microbial Fuel Cells, John Wiley & Sons, Inc., Hoboken, NJ, 2007.
[3] R.A. Rozendal, H.V.V. Hamelers, C.J.N. Guisman, Environ. Sci. Technol. 40 (2006) 5206–5211.
[4] J.R. Kim, S. Cheng, S.-E. Oh, B.E. Logan, Environ. Sci. Technol. 41 (2007) 1004–1009.
[5] H. Liu, B.E. Logan, Environ. Sci. Technol. 38 (2004) 4040–4046.
[6] W.-W. Li, G.-P. Sheng, X.-W. Liu, H.-Q. Yu, Bioresour. Technol., doi:10.1016/j.biortech.2010.03.090.
[7] F. Harnisch, U. Schroder, F. Scholz, Environ. Sci. Technol. 42 (2008) 1740–1746.
[8] Y. Zuo, S. Cheng, B.E. Logan, Environ. Sci. Technol. 42 (2008) 6967–6972.
[9] R. Rozendal, H.V.M. Hamelers, R.J. Molenkamp, C.J.N. Buisman, Water Res. 41 (2007) 1984–1994.
[10] L. Zhuang, C. Feng, S. Zhou, Y. Li, Y. Wang, Process Biochem. 45 (2010) 929–934.
[11] F. Zhao, F. Harnisch, U. Schroder, F. Scholz, P. Bogdanoff, I. Herrmann, Environ. Sci. Technol. 40 (2006) 5193–5199.
[12] T.H.J.A. Sleutels, H.V.M. Hamelers, R.A. Rozendal, C.J.N. Buisman, Int. J. Hydrogen Energy 34 (2009) 3612–3620.
[13] F. Harnisch, U. Schröder, ChemSusChem 2 (2009) 921–926.
[14] X. Zhang, S. Cheng, X. Wang, X. Huang, B.E. Logan, Environ. Sci. Technol. 43 (2009) 8456–8461.
[15] Y. Fan, H. Hu, H. Liu, J. Power Sources 171 (2007) 348–354.
[16] X. Zhang, S. Cheng, X. Huang, B.E. Logan, Biosens. Bioelectron. 25 (2010) 1825–1828.
[17] M.R. Hibbs, M.A. Hickner, T.M. Alam, S.K. McIntyre, C.H. Fujimoto, C.J. Cornelius, Chem. Mater. 20 (2008) 2566–2573.
[18] M. Mehanna, T. Saito, J. Yan, M. Hickner, X. Cao, X. Huang, B.E. Logan, Energy Environ. Sci. 3 (2010) 1114–1120.
[19] T. Saito, M.D. Merrill, V.J. Watson, B.E. Logan, M.A. Hickner, Electrochim. Acta 55 (2010) 3398–3403.
[20] T. Saito, T.H. Roberts, T.E. Long, M. Hickner, B.E. Logan, Energy Environ. Sci., 2010, doi:10.1039/c0ee00229a.
[21] S. Cheng, H. Liu, B.E. Logan, Electrochem. Commun. 8 (2006) 489–494.
[22] Y. Feng, Q. Yang, X. Wang, B.E. Logan, J. Power Sources 195 (2010) 1841–1844.
[23] O. Bretschger, A. Obraztsova, C.A. Sturm, I.S. Chang, Y.A. Gorby, S.B. Reed, D.E. Culley, C.L. Reardon, S. Barua, M.F. Romine, J. Zhou, A.S. Beliaev, R. Bouhenni, D. Saffarini, F. Mansfeld, B.-H. Kim, J.K. Fredrickson, K.H. Nealson, Appl. Environ. Microbiol. 73 (2007) 7003–7012.
[24] B.E. Logan, P. Aelterman, B. Hamelers, R. Rozendal, U. Schröder, J. Keller, S. Freguiac, W. Verstraete, K. Rabaey, Environ. Sci. Technol. 40 (2006) 5181–5192.
[25] S. Cheng, H. Liu, B.E. Logan, Environ. Sci. Technol. 40 (2006) 2426–2432.
[26] Z. He, N. Wagner, S.D. Minteer, L.T. Angenent, Environ. Sci. Technol. 40 (2006) 5212–5217.